

# An ancient and impure frozen ocean on Ceres implied by its ice-rich crust

Received: 13 July 2023

Accepted: 29 July 2024

Published online: 18 September 2024

 Check for updates

I. F. Pamerleau<sup>1</sup>✉, M. M. Sori<sup>1</sup> & J. E. C. Scully<sup>2</sup>

Ceres is a key object in understanding the evolution of small bodies and is the only dwarf planet to have been orbited by a spacecraft, NASA's Dawn mission. Dawn data paint an inconclusive picture of Ceres' internal structure, composition and evolutionary pathway: crater morphology and gravity inversions suggest an ice-rich interior, while a lack of extensive crater relaxation argues for low ice content. Here we resolve this discrepancy by applying an ice rheology that includes effects of impurities on grain boundary sliding to finite element method simulations of Cerean craters. We show that Ceres can maintain its cratered topography while also having an ice-rich crust. Our simulations show that a crust with ~90% ice near the surface, which gradually decreases to 0% at 117 km depth, simultaneously matches the observed lack of crater relaxation, observed crater morphology and gravity inversions. This crustal structure results from a frozen ocean that became more impurity rich as it solidified top-down. Therefore, the Dawn data are consistent with an icy Ceres that evolved through freezing of an ancient, impure ocean.

Dwarf planet Ceres is thought to have a high ice content compared with other objects in the inner solar system<sup>1,2</sup>. Constraining the composition of Ceres' interior helps to elucidate its internal processes, differentiation state and potential habitability. Although ice is unstable on the surface of Ceres owing to its proximity to the Sun, hydrated minerals were spectroscopically observed on the dwarf planet's surface before the arrival of the National Aeronautics and Space Administration (NASA)'s Dawn mission<sup>3</sup>. It was thought that these hydrates would act as an insulating regolith for an extremely ice-rich crust below, which was suggested from pre-Dawn density measurements<sup>4</sup>. Because of these observations and the inferred crustal composition, it was predicted that Ceres would be unable to support topography if it was fully differentiated with complete ice–rock separation<sup>5</sup>. These models suggested that craters on an icy Ceres would efficiently viscously relax away over geologic time.

When Dawn arrived at Ceres, some data were consistent with the hypothesis that the body contains an ice-rich crust, and some data were not. Gravity inversions<sup>6</sup> implied an average crustal density ( $1,287 \text{ kg m}^{-3}$ ) very near that of water ice, and nuclear spectroscopy revealed high amounts of hydrogen in the upper metre, which is

consistent with expansive water ice below the regolith<sup>7</sup>. Additionally, the simple-complex transition diameter of Cerean craters places it along the trend of other icy bodies<sup>8</sup>, suggesting that craters form as if in an ice-rich crust. There have also been many geomorphologic observations that support the presence of subsurface ice<sup>9</sup>. However, it has been argued that the heavily cratered landscape revealed by Dawn on Ceres today is inconsistent with an icy internal structure<sup>10</sup>. Numerical modelling suggested that the lack of extensive crater relaxation implied Ceres' crust has no more than 40% ice volumetrically<sup>11</sup>. Therefore, the current accepted interior structure invokes weak differentiation, with a crustal composition that is less than 40% ice, with silicates, salts, organic material and clathrates making up the rest of the material<sup>11,12</sup>.

Although consistent with unrelaxed craters, there are potential issues with an ice-poor, weakly differentiated Ceres. This structure relies on the idea that even a low ice content will allow craters to form in the same manner they do in extremely ice-rich bodies like the icy Galilean satellites, but it is unknown how low the ice content can be for this to still hold true. Additionally, the current model invokes clathrates, a light but strong material formed when gas is trapped in an ice lattice. Clathrates were thought to be necessary to account for the

<sup>1</sup>Department of Earth, Atmospheric and Planetary Science, Purdue University, West Lafayette, IN, USA. <sup>2</sup>Jet Propulsion Laboratory, California Institute of Technology, Pasadena, CA, USA. ✉e-mail: [ipamerle@purdue.edu](mailto:ipamerle@purdue.edu)

lack of relaxation and low density of the crust, but it is uncertain if they would form on Ceres based on thermochemical models<sup>12</sup>. Moreover, clathrates may be unstable in the presence of salts<sup>13</sup>, which are abundant on Ceres: brines at depth that have erupted onto the surface have been proposed as the source of the faculae in Occator crater<sup>14–16</sup> and the cryovolcanic construct Ahuna Mons<sup>17</sup>. Lastly, it is unknown if an interior structure for Ceres with only weak differentiation between ice and rock is realistic<sup>10,18</sup>. Ceres' crust may have formed from a freezing ocean<sup>12,19–21</sup>, and thermal models have suggested that efficient separation of water and silicates would have occurred early in Ceres' history<sup>1,4,22</sup>, leading to a strongly differentiated interior. Ice shells on other ocean worlds are thought to be extremely ice rich, like on Europa and Enceladus. Callisto has been proposed to only be partly differentiated<sup>23</sup> with a subsurface ocean<sup>24</sup>, but other work has argued that, like Ceres, an undifferentiated or only partially differentiated Callisto would be very surprising on theoretical grounds<sup>25</sup>. Note that we use 'differentiation' in this Article to refer to separation of rock and water ice and does not necessarily include metal.

We propose that an ice-rich crust that is mechanically strong fits Dawn data and numerical models of Ceres' thermal evolution. Rheologic experiments conducted after Dawn's arrival at Ceres have shown that ice can behave much more rigidly on geologic timescales than previously thought with only a small ( $\geq 6\%$ ) impurity content<sup>26,27</sup>. This more rigid ice rheology is highly relevant to Ceres given that the gravity inversions are consistent with an icy crust with minor impurity content. However, this rheology has not yet been applied to Ceres. We hypothesize that, when this rheology is considered, Ceres can maintain its cratered landscape even with an icy crust and differentiated interior. A mechanically strong, icy crust would fit the Dawn data without invoking clathrates or the low-ice crater formation theory. While this is a 'simpler' way to reconcile Ceres' low-density crust and cratered landscape, it does not exclude the structure currently in the literature<sup>10–12</sup>.

We tested our hypothesis by simulating relaxing Cerean craters using a finite element method (FEM) model. We used COMSOL Multiphysics software to construct our model and assessed the interior structures that could allow craters to be maintained. Viscoelastic relaxation is dependent on three main parameters in our model: crater diameter (large craters relax faster than small ones), latitude (a proxy for temperature, which strongly affects rheology) and crustal ice content (icier materials relax faster than drier materials). The annual-average temperature is calculated to be  $-156$  K at the equator and  $-90$  K at the poles<sup>28</sup>. We seek to maximize the ice content while minimizing relaxation because, other than the lack of widespread relaxation<sup>10,11</sup>, the Dawn data suggest an icy crust<sup>6–9</sup>. More details about the FEM model can be found in Methods.

We tested three basic crustal structures in our FEM simulations to assess which structures could maintain craters and be consistent with the heavily cratered landscape observed by Dawn. The first structure is a uniform crust, such that ice and impurity content are uniform throughout space for each simulation (Fig. 1a). A uniform crustal structure could be a result of a partially differentiated Ceres that did not fully separate the rock and ice material, either due to a strong, undifferentiated crust that received little accretional heat<sup>19</sup> or a frozen ocean rich in fines<sup>20,21</sup>. The second internal structure we investigated was a two-layer crust (Fig. 1b). The layers are of uniform compositions, and the less dense layer (that is, with a higher ice content and weaker rheology) is on top of a denser, drier layer. A two-layer model does not fit a proposed internal evolution pathway for Ceres but serves as a useful conceptual example to help us understand how discrete changes in the distribution of impurities affect relaxation. Larger craters are more sensitive to material deeper in the interior. Therefore, higher impurity content with depth may help to slow down relaxation of larger craters relative to the uniform case. For both this and the first crustal scenarios, the total crustal thickness<sup>6</sup> is 40 km. Lastly, we tested a gradational crustal structure on Ceres, where the shallow subsurface

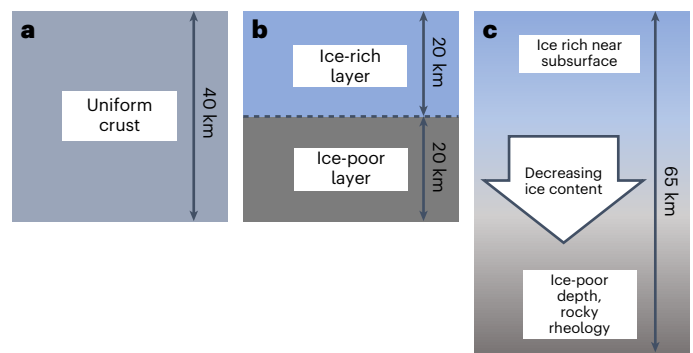


**Fig. 1 | Schematic of simulated crustal structures.** **a**, A uniform crust, 40 km thick. **b**, A two-layer crust, where the top layer is icier than the bottom layer. Each layer is 20 km in our simulations. **c**, The gradational crust, in which the ice content decreases linearly with depth. The uniform crust in **a** would need to be more impurity rich than the top layer and more ice-rich than the bottom layer of **b** for both scenarios to match Dawn gravity inversions. The composition gradient in **c** depends on the ice content in the near subsurface to match gravity inversions.

has a high ice content that gradually decreases with depth as impurity content increases (Fig. 1c). Like the two-layer scenario, this structure has more impurities with depth, impeding relaxation of large craters. Our nominal structure for this scenario contains 90% ice near the surface and linearly decreases to 0% ice at 117 km depth. This structure yields an average density of the top 41 km that matches gravity inversions<sup>6</sup>. We note that other surface ice contents and impurity gradients can be chosen to be consistent with Dawn data, given the uncertainty in the gravity inversions and the densities of the impurities. This gradational internal structure could be the result of a top-down ancient frozen ocean on Ceres that contained impurities over a range of grain sizes. In this scenario, fine-grained impurities were trapped between the ice grains<sup>12,20</sup> as freezing progressed, while slightly larger grains remained below the freezing front, which led to an ocean that became more impurity rich with time and depth. This would result in a crust that becomes denser with depth, consistent with gravity measurements made by the Dawn spacecraft<sup>29</sup>.

## Results

Our model predicts negligible crater relaxation for much of the parameter space, regardless of the simulated crustal structure. For all crustal structures, simple craters ( $\leq 12$  km in diameter) are retained ubiquitously under all conditions as long as  $\geq 6\%$  impurities exist. For example, a 12-km-diameter crater at the warm equator in a crust that is uniformly 90% ice relaxes by  $< 5\%$  (see Methods for the definition of 'per cent relaxation') after 1 Gyr (Fig. 2). Simple craters at other latitudes, in crusts of lower ice content, or of smaller diameter relax even less. These findings are a major divergence from previous work, which argued that even simple craters on Ceres would relax away in an ice-rich crust<sup>5,11</sup>.

The relaxation of complex craters is dependent on free parameters and assumed crustal structure. Complex craters  $\leq 40$  km in diameter experience little deformation on Gyr timescales in the cold temperatures of the mid- or high latitudes in ice-rich crusts (Fig. 3). However, large complex craters at the warm, equatorial latitudes experience substantial amounts of relaxation for some crustal structures. A uniform-composition crust allows  $\sim 30\%$  relaxation at the equator for 40-km-diameter craters in a 90% ice crust (Fig. 3a). Increasing impurity content will hinder relaxation but also could increase the crustal density to a value inconsistent with gravity inversions if the impurities are in the form of dense silicates. The two-layer crustal structure yields similar results to the uniform crust case because craters are most sensitive to the top layer's composition even for our largest simulated craters. Holding the ice content of the top layer constant and varying the ice content of the bottom layer yields nearly identical relaxation

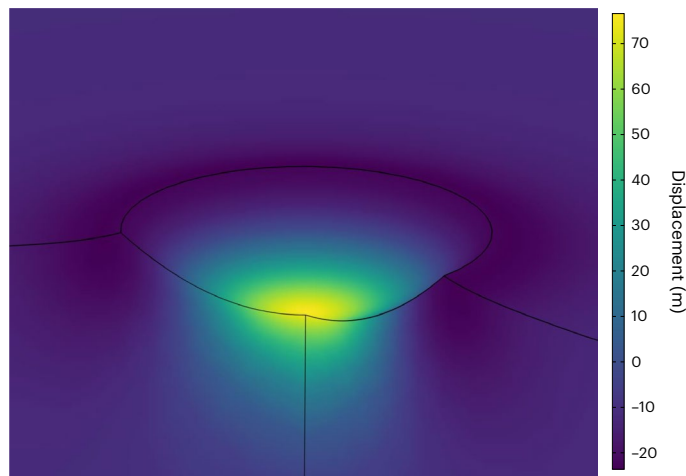


**Fig. 2 | Simulated 12-km-diameter crater showing vertical displacement.**

This simulation was run in a uniformly 90% ice crust (Fig. 1a) at the equator and shows total vertical displacement after 1 Gyr of relaxation. The black lines are the initial state of the simulation, and the solid colour shows the final state of the simulation. In this case, the crater has only shallowed by ~70 m from an initial depth of 2,400 m (seen as the solid colour at the centre of the crater slightly offset from the black line), for a relaxation percentage of <4%.

states. The two-layer scenario yields slightly lower relaxation percentages compared with the uniform crust case for larger craters, which are relatively more sensitive to the deeper layer composition (Fig. 3a,b). The last scenario, a crust nominally with 90% ice near the surface and becoming gradually more impurity rich with depth, yields substantially less relaxation for large craters compared with a uniform or two-layer crust. Complex craters between 12 and 40 km in diameter relax by <20% after 1 Gyr depending on latitude and crater size (Fig. 3c). As is the case with the other simulated crustal structures, the higher the impurity content, the less relaxation is allowed, but the density profile is also changed. Displacement and per cent relaxation values of our simulations in Fig. 3 can be found in Supplementary Data 1.

## Discussion

All crustal structures we tested yield substantially less relaxation of craters on Ceres than previously thought possible in an ice-rich crust, as long as a few per cent or more of impurities are present. This result occurs because impurities effectively prevent grain boundary sliding (GBS)<sup>26</sup>, a major deformation mechanism of ice on Ceres at the relevant temporal and spatial scales. The distribution and quantity of these impurities can help to minimize relaxation of large, equatorial craters, which will help determine our favoured crustal structure. A uniform crust with a high ice content (90%) is able to retain craters throughout most of the parameter space (that is, crater diameter and latitude). Simple craters and small complex craters will never relax on Ceres as long as a few per cent or more of impurities are present, as the largest simple crater in the warmest plausible temperature experiences <5% relaxation after 1 Gyr (Fig. 2). However, a uniformly icy crust allows more relaxation of large, equatorial craters than is observed on Ceres. Increasing impurity content will slow down relaxation to better fit observed Cerean craters (for example, Supplementary Data 2), but with too high of an impurity content, the crustal structure would not fit gravity data<sup>6</sup>. The simulated uniform crust that most closely matches observed gravity inverted density measurements (~75% ice) yields 23% relaxation for a 40 km crater at the equator (Supplementary Data 2). Although a uniform crustal structure does not perfectly match the observations of the cratered terrain on Ceres, it allows for an ice-rich crust that retains topography more efficiently than previously thought<sup>5,10,11</sup>. The two-layer model simulations do not fit the Dawn data as well as the uniform crust. Two-layer simulations perform slightly better (that is, have lower

per cent relaxations) than uniform simulations when the top layer and uniform crust share the same composition. However, this small improvement in matching the observed rheology is outweighed by the large increase in density from the lower, more impurity-rich layer. Increasing the impurity content of a uniform crust will cause less relaxation to occur than keeping the impurity content fixed and adding a higher impurity second layer. Therefore, a uniform crustal structure should fit both the lack of extensive crater relaxation<sup>10,11</sup> and density profile<sup>6</sup> measured from the Dawn mission better than a two-layer model.

We argue that a crust with high ice content at the surface that grades into lower ice content at depth best matches Dawn observations (Fig. 1c). Our preferred model has an extremely ice-rich near subsurface at 90% and linearly decreases in ice content until it reaches 0% ice at 117 km depth. This crustal structure minimizes crater relaxation (Fig. 3) and is consistent with Ceres' cratered landscape<sup>8</sup>, crater morphologies<sup>8</sup>, high hydrogen content in the shallow subsurface<sup>7</sup>, icy geomorphology<sup>9</sup> and increasing density with depth<sup>29</sup>, all without invoking clathrates. This gradational structure also allows for enough water ice at depth to create the brines hypothesized to form the bright faculae in Occator crater, which probably require endogenic H<sub>2</sub>O (refs. 14,15). We tested other uniform and gradational ice/impurity contents (with greater fractions of impurities) and found that it takes a substantial increase in impurity content to reduce relaxation by <10% (see Supplementary Data 2 for examples). As this dramatic increase in higher density impurities does not match gravity inversions and only slightly minimizes the relaxation, we favour a crustal composition of 90% ice at the surface and 0% ice at 117 km depth because these values match gravity inversions that suggest an average density<sup>6</sup> in the upper 41 km of 1,287 kg m<sup>-3</sup>.

Fine-grained impurities need to be trapped at the ice grain boundaries to inhibit GBS<sup>26</sup> and make ice sufficiently resistant to relaxation over long timescales, ruling out a scenario of a pure ice crust. Soluble impurities such as salts and carbonates are viable candidates to freeze out with the ice<sup>12</sup> and increase the crust's strength. Colloidal solutions (fine, insoluble particles suspended in solution) have been suggested to help trap impurities in a fine-rich fluid<sup>30,31</sup>, which has been proposed to account for the impurities in Ceres' ancient ocean<sup>20</sup>. Experimental data suggest that lenses of fine-grained impurities and ice may occur on Earth, as the trapping of impurities between ice grains has been observed in terrestrial lake settings<sup>32</sup> and Antarctic ice<sup>33</sup>, and the same thing very well may have occurred on Ceres. Both soluble impurities and suspended colloidal solutions may work in tandem to help trap impurities between ice grains and increase the strength of Ceres' crust, as we simulate in our models.

These different crustal structures may reflect different evolutionary pathways for Ceres and its ancient ocean. There are four main proposed internal structures for Ceres. The first is an undifferentiated body<sup>34</sup> with no melting of water ice. The second is a partially differentiated three-layer Ceres with an undifferentiated crust being maintained over a warmer, differentiated mantle and core<sup>19</sup>. Both of these cases are represented by our uniform crustal scenario (Fig. 1a) and are not favoured. The other two evolutionary pathways involve full melting of the water ice, leading to a mudball Ceres<sup>19–21</sup> or a brine-rich Ceres. In the mudball theory, the accreted, undifferentiated ice melts from the inside out owing to short-term radiogenic heating and leaves an ocean rich with suspended fine-grained particles. In this 'muddy ocean', larger clasts (≥mm) will sink rather quickly through the ocean to form a rocky core, but fines (<μm) will be suspended over long periods of time, if not indefinitely<sup>20,21</sup>. As the muddy ocean freezes top-down, the fines are trapped in the forming crust. In the brine-rich theory, a freezing ocean may form with increasing impurities (be it salts, clathrates or suspended particles) with depth<sup>12</sup>, which matches gravity inversions from Dawn's second extended mission suggesting an increasing density with depth<sup>29</sup>. A leftover brine layer may be present in this pathway, and the core could contain both water ice and rock. The

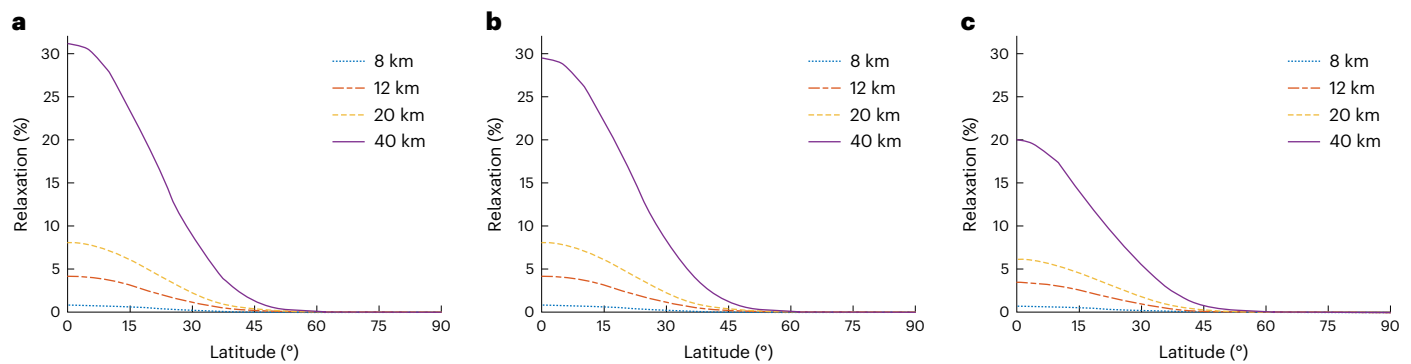


**Fig. 3 | Per cent relaxation versus latitude for different crater sizes in our three crustal structures. a,** A uniform crust with  $\sim 90\%$  ice content, 40 km thick (Fig. 1a). **b,** A two-layer crust, where a  $\sim 90\%$  ice layer overlies a  $\sim 63\%$  ice layer, both 20 km thick (Fig. 1b). **c,** A gradational crust, with  $\sim 90\%$  ice in the near subsurface

and  $\sim 40\%$  ice at 65 km depth, the bottom of the simulated crust (Fig. 1c).

A 40 km crater at the equator (purple, solid line) experiences the least amount of relaxation ( $\sim 20\%$ ) in this crustal structure.

main difference between the mudball theory and the brine-rich Ceres is the lack of a brine-rich layer between the crust and core in a mudball Ceres, as well as a purely rocky core in the mudball and a water/rock core in the brine-rich Ceres. Note that while increasing impurities with depth explains the Dawn gravity inversions<sup>29</sup>, decreasing porosity in a uniform crust would also explain this observation. Our gradational crustal structure agrees with the top-down freezing ocean model and the observed density profile. Regardless of the mechanism of crustal formation, our results show that either method can allow more ice than previously thought, making Ceres more similar to other ocean worlds with ice-rich shells.

Our results imply that previous geophysical studies of Ceres may need to be revisited with the interior structure that we favour, an ice-rich compositionally gradient crust, in mind. Previous work suggested that Dawn data allow Ceres to be only weakly<sup>10,18</sup> or even not differentiated at all<sup>34</sup> based on topographic support arguments. However, our proposed interior structure with a strong, impure-ice crust implies efficient separation of water from silicates that later formed a compositional gradient because of top-down freezing. This is consistent with thermal evolution models that predict water–silicate separation on Ceres is efficient and inevitable<sup>22</sup>. Deformation models of mounds that may have formed cryovolcanically<sup>28,35</sup> or from solid-state flow<sup>36</sup> may overestimate their formation rates if the material comprising these features has  $\geq 6\%$  impurity content.

We simulated craters up to 40 km in diameter because they have been efficiently retained on Ceres. Craters larger than this tend to have more complicated morphologies<sup>9</sup> that are asymmetric. Additionally, we observed subtle signs of relaxation for Cerean craters in the 50–100 km range (Supplementary Fig. 1 and Supplementary Section I). As the nature of this relaxation is asymmetric, it is not appropriate to simulate their deformation in our two-dimensional (2D) axisymmetric models. While we do not simulate larger craters in this work, our gradational crust will help minimize their relaxation because bigger craters will be more sensitive to deeper, more impurity-rich material. Further, some of the largest craters on Ceres cited with deep floors ( $>4$  km) indicating little to no relaxation has occurred (for example, Vinotonus, Ezinu, Urvara and Yalode) are found at mid-latitudes ( $\sim 45^\circ$ )<sup>8</sup>, where our simulations show relaxation will be ineffective regardless of crater diameter because of cold surface temperatures (Fig. 3). For craters  $>100$  km, there is evidence that substantial relaxation has occurred from the dearth of large craters<sup>37</sup> and topographic power spectra<sup>6</sup>. Impact and relaxation simulations focused on planetary-scale basins could further help elucidate the evolutionary pathway of Ceres' ancient ocean.

Our proposed interior structure and evolutionary pathway for Ceres has implications for future spacecraft missions and can be tested by those missions. As a relic ocean world in the inner solar system, Ceres

is often treated as an accessible analogue to other, more traditional ocean worlds<sup>38,39</sup> (for example, the icy Galilean moons). If the ancient ocean froze out to form a crust with a high ice content, it is possible that Ceres is less of an outlier and more akin to other ocean worlds than previously thought. Future mission concepts<sup>40</sup> could test this idea by inferring the compositional structure of the upper few kilometres with geophysical methods or constraining Ceres' thermal evolution through returned sample analysis. Ground-penetrating radar may help determine the ice content of Ceres' crust and any lateral and vertical variability, which would elucidate which crustal model best agrees with Ceres' interior. Additional key objectives of a future mission to Ceres, such as identifying the rock–ocean interface where brines are present<sup>40</sup>, may need to be reassessed with our proposed interior structure in mind. In our model, the interface between the base of the crust–ice shell and any remnant brines may be deeper than in current models<sup>6</sup>.

## Methods

We use the FEM software COMSOL Multiphysics to run our viscoelastic simulations. We use the thermal physics module to set up a temperature profile through the interior and the solid mechanics module to simulate relaxation.

We simulated three crustal structures in this work: a uniform, 40-km-thick crust (90% ice in Fig. 3a); a two-layer crust, where each layer is 20 km thick and has a uniform composition (90% and 63% ice for the top and bottom layer in Fig. 3b, respectively); and a gradational crust that decreases in ice content with depth. We propose a gradient that consists of 90% ice at the near subsurface, linearly grading to 0% ice at 117 km depth (Fig. 3c). We only simulate this crust to a depth of 65 km (Fig. 1c) as the material below that will have  $<40\%$  ice and deformation will be effectively inhibited<sup>11</sup>. We favour the gradational crust as it best fits Dawn data of all our simulations (see Discussion for more details). However, we only use ice and hydrated silicates in the composition of our simulations, and the values for these crustal structures have some flexibility based on this assumption. We also simulated other, more impurity-rich compositions for these three scenarios, which are reported in Supplementary Data 2.

## Geometry

We construct our simulations to be realistic while being computationally inexpensive. We model simple craters ( $\leq 12$  km in diameter) with a parabolic bowl shape geometry<sup>41</sup>. The floor elevation is one-fifth the diameter below the surrounding terrain. A topographic profile of a young Cerean crater is used for the complex crater simulations and is taken from Dawn observations. The topography is of a 40 km crater and used unaltered for our 40 km simulations, but we scale it on the basis of the depth-diameter ratios reported in ref. 8 for our 20 km simulation.

Figure 2 shows a detail of a portion of a 12-km-diameter crater simulation, but the actual model domain for each simulation continues radially outwards to minimize effects from the lateral boundaries on the crater (for three and six crater diameters from the centre of the crater for complex and simple craters, respectively). The crust extends to a depth of 40 km for the uniform and two-layer crustal structures (Fig. 1a,b), as suggested by gravity data<sup>6</sup>, or 65 km for the gradational crust case (Fig. 1c), below which the crust has low enough ice content such that it only deforms in a rocky manner<sup>11</sup>.

The simulations are 2D axisymmetric, as the craters we simulate in this work are largely radially symmetric. This geometry assumes that any features that are not radially symmetric in these craters are not big enough to affect the viscoelastic relaxation of the overall crater. This would not be the case for craters >40 km, which show features sure as fractured floors, central pits and so on<sup>8</sup> that would need to be simulated in a three-dimensional asymmetric simulation. The mesh is designed to be finer near the crater, where deformation is maximized, than elsewhere in the domain. We tested a few cases and found that our results do not notably change by increasing the resolution of the mesh compared with the simulations presented here.

### Thermal model

As the rheology of the simulated material is highly dependent on temperature, we calculate an initial thermal profile through the interior before allowing deformation. The model uses the geothermal heat flow, surface temperature and thermal material properties to calculate temperature through the crust. The heat flow is taken to be  $1 \text{ mW m}^{-2}$ , but we note that increasing the value to  $3 \text{ mW m}^{-2}$  did not substantially affect our results. The temperature boundary condition at the top is the annual-average surface temperature, justified by the fact that the thermal skin depth is orders of magnitude smaller than the crustal thickness. That surface temperature is latitudinally dependent and taken from a previous thermal model<sup>28</sup>, which assumes an emissivity of 0.9. We calculate the surface temperature every  $5^\circ$  latitude to apply a thermal boundary condition to our simulations. The surface temperature at the equator is estimated to be  $-156 \text{ K}$ , while the surface temperature at the poles is estimated to be  $-90 \text{ K}$ . We assume a thermal conductivity equation for all simulations that is a linearly weighted mixture of ice and impurities, depending on temperature and the impurity content in that simulation. Therefore, a uniform crust will have a thermal conductivity that is only temperature dependent for each simulation, and similarly for each layer in the two-layer model. The gradational crust will have a thermal conductivity that depends on both temperature and composition, as temperature and impurity content change with depth. Ice has a temperature-dependent thermal conductivity<sup>42</sup> of  $651 \text{ W m}^{-1} \text{ K}^{-1}$ , where  $T$  is temperature in Kelvin, and the impurities have thermal conductivity<sup>43</sup> of  $2 \text{ W m}^{-1} \text{ K}^{-1}$ . We note that, while the thermal conductivity depends on the impurity content (which varies with depth for the gradational scenario), the thermal gradient through all simulated crusts differs by only a few Kelvin owing to Ceres' low heat flow. For example, the temperature at 40 km depth below the equator is 166, 167 and 168 K for each crustal structure from Fig. 3, respectively. We do not account for insulating regolith, which may allow a few more Kelvin in the near subsurface.

### Viscoelastic relaxation

Our simulations include both elastic and viscous deformation. Elastic deformation in our model is controlled by Young's modulus and Poisson's ratio, assumed to be  $10^{10} \text{ Pa}$  and 0.25, respectively. Elastic deformation is small on geological timescales; our results are not sensitive to small changes in the elastic parameters.

Viscous deformation is the dominant control on whether craters are maintained over geological timescales. For the viscous creep physics, we solve the Stokes equations for conservation of mass and momentum, respectively:

$$\nabla \mathbf{u} = 0 \quad (1)$$

$$\nabla \boldsymbol{\sigma} + \rho \mathbf{g} = 0, \quad (2)$$

where  $\mathbf{u}$  is the velocity vector,  $\boldsymbol{\sigma}$  is the Cauchy stress tensor,  $\rho$  is the density ( $917 \text{ kg m}^{-3}$  for ice,  $2,500 \text{ kg m}^{-3}$  for impurities) and  $\mathbf{g}$  is the acceleration due to gravity vector ( $0.27 \text{ m s}^{-2}$  on Ceres).

Viscous relaxation of craters in an icy material is driven by several deformation mechanisms. At the stresses and timescales relevant to kilometre-scale or larger topography on Ceres<sup>35</sup>, the two important mechanisms are dislocation creep<sup>44</sup> and GBS<sup>45</sup>, given by the following two equations, respectively:

$$\dot{\epsilon}_{\text{disl}} = 10^{5.1} e^{-8\varphi - \frac{61,000}{RT}} \tau^4 \quad (3)$$

$$\dot{\epsilon}_{\text{GBS}} = 10^{-2.4} e^{-3.6\varphi - \frac{49,000}{RT}} \tau^{1.8} d^{-1.4}, \quad (4)$$

where  $\dot{\epsilon}$  is the strain rate,  $\tau$  is the deviatoric stress in MPa,  $\varphi$  is the fractional impurity content,  $T$  is the temperature in Kelvin,  $R$  is the gas constant and  $d$  is the grain size in metres. Note that the addition of particulates into an ice mass is accounted for with a factor of  $e^{(-b\varphi)}$  where  $b$  is a constant,  $b=2$ . This factor also has a power relation (for example, ref. 11), leading to the  $e^{(-8\varphi)}$  factor in equation (3). COMSOL describes deviatoric stress with the von Mises equivalent stress, which is volume preserving and is adjusted for the uniaxial strain conditions in which these values were experimentally derived. These temperature-, stress- and composition-dependent rheology equations are applied throughout all simulations, but with an impurity content of  $\geq 6\%$  (ref. 26), GBS is made ineffective<sup>26</sup>, leaving dislocation creep as the important deformation mechanism. Dislocation creep is grain size independent<sup>45</sup>, and so we do not assume a particular grain size. GBS would be the dominant deformation mechanism for the Cerean craters in pure ice, so without it, a crust with  $\geq 6\%$  impurities is much stronger than previously modelled. Other equations for strain rates of these deformation mechanisms have been proposed<sup>45</sup> and may result in slightly different strain rate values.

At the end of the simulations (1 Gyr of deformation), we calculate the per cent relaxation of the crater. We define 'per cent relaxation' as the ratio of the difference in elevation between the crater rim and floor at the beginning and end of the simulation, where 0% reflects no change in elevation. For simple craters, we define the floor elevation as the centre of the crater, which is one-fifth the diameter of the crater. Complex craters have relatively flat floors, but for the topographic profiles we used in our simulations, there is a slight slope down towards the centre of the crater. We define the floor elevation of the complex craters as the elevation where the relatively flat floor and peak meet, which is the deepest part of the crater. We note that the floor elevation is the deepest part of the crater in each simulation, and because of this, will have the highest stresses (and displacement).

The surface of the model, including the crater and surrounding terrain, is set to be a free surface. The bottom surface is fixed, and the wall that is not being rotated around (to make the model 2D axisymmetric) is allowed to deform in the  $z$  direction but not the  $r$  direction.

### Data availability

Data from NASA's Dawn mission are available to the public in the NASA Planetary Data System's small bodies node (<https://pds-smallbodies.astro.umd.edu/>).

### Code availability

The code used to simulate relaxing craters is available on Figshare at [https://figshare.com/projects/An\\_ancient\\_and\\_impure\\_frozen\\_ocean\\_on\\_Ceres\\_implied\\_by\\_its\\_ice-rich\\_crust/210268](https://figshare.com/projects/An_ancient_and_impure_frozen_ocean_on_Ceres_implied_by_its_ice-rich_crust/210268). The code was made in the COMOSL Multiphysics Software and requires a licence for

the software, as well as the Solid Mechanics and Nonlinear Materials modules.

## References

- Castillo-Rogez, J. C. & McCord, T. B. Ceres' evolution and present state constrained by shape data. *Icarus* **205**, 443–459 (2010).
- Thomas, P. C. et al. Differentiation of the asteroid Ceres as revealed by its shape. *Nature* **437**, 224–226 (2005).
- Milliken, R. E. & Rivkin, A. S. Brucite and carbonate assemblages from altered olivine-rich materials on Ceres. *Nat. Geosci.* **2**, 258–261 (2009).
- McCord, T. B. & Sotin, C. Ceres: evolution and current state. *J. Geophys. Res. Planets* **110**, 1–14 (2005).
- Bland, M. T. Predicted crater morphologies on Ceres: probing internal structure and evolution. *Icarus* **226**, 510–521 (2013).
- Ermakov, A. I. et al. Constraints on Ceres' internal structure and evolution from its shape and gravity measured by the Dawn spacecraft. *J. Geophys. Res. Planets* **122**, 2267–2293 (2017).
- Prettyman, T. H. et al. Extensive water ice within Ceres' aqueously altered regolith: evidence from nuclear spectroscopy. *Science* **355**, 55–59 (2017).
- Hiesinger, H. et al. Cratering on Ceres: implications for its crust and evolution. *Science* **353**, aaf4759 (2016).
- Sizemore, H. G. et al. A global inventory of ice-related morphological features on dwarf planet Ceres: implications for the evolution and current state of the cryosphere. *J. Geophys. Res. Planets* **124**, 1650–1689 (2019).
- Fu, R. R. et al. The interior structure of Ceres as revealed by surface topography. *Earth Planet. Sci. Lett.* **476**, 153–164 (2017).
- Bland, M. T. et al. Composition and structure of the shallow subsurface of Ceres revealed by crater morphology. *Nat. Geosci.* **9**, 538–542 (2016).
- Castillo-Rogez, J. et al. Insights into Ceres's evolution from surface composition. *Meteorit. Planet. Sci.* **53**, 1820–1843 (2018).
- Safi, E. et al. Properties of CO<sub>2</sub> clathrate hydrates formed in the presence of MgSO<sub>4</sub> solutions with implications for icy moons. *Astron. Astrophys.* **600**, A88 (2017).
- Scully, J. E. C. et al. The varied sources of faculae-forming brines in Ceres' Occator crater emplaced via hydrothermal brine effusion. *Nat. Commun.* **11**, 3680 (2020).
- Raymond, C. A. et al. Impact-driven mobilization of deep crustal brines on dwarf planet Ceres. *Nat. Astron.* **4**, 741–747 (2020).
- Russell, C. T. et al. Dawn arrives at Ceres: exploration of a small, volatile-rich world. *Science* **353**, 1008–1010 (2016).
- Ruesch, O. et al. Cryovolcanism on Ceres. *Science* **353**, aaf4286 (2016).
- Park, R. S. et al. A partially differentiated interior for (1) Ceres deduced from its gravity field and shape. *Nature* **537**, 515–517 (2016).
- Neumann, W., Jaumann, R., Castillo-Rogez, J., Raymond, C. A. & Russell, C. T. Ceres' partial differentiation: undifferentiated crust mixing with a water-rich mantle. *Astron. Astrophys.* **633**, A117 (2020).
- Travis, B. J., Bland, P. A., Feldman, W. C. & Sykes, M. V. Hydrothermal dynamics in a CM-based model of Ceres. *Meteorit. Planet. Sci.* **53**, 2008–2032 (2018).
- Neveu, M. & Desch, S. J. Geochemistry, thermal evolution, and cryovolcanism on Ceres with a muddy ice mantle. *Geophys. Res. Lett.* **42**, 10197–10206 (2015).
- Castillo-Rogez, J. C. Ceres—neither a porous nor salty ball. *Icarus* **215**, 599–602 (2011).
- Anderson, J. D. et al. Shape, mean radius, gravity field, and interior structure of Callisto. *Icarus* **153**, 157–161 (2001).
- Khurana, K. K. et al. Induced magnetic fields as evidence for subsurface oceans in Europa and Callisto. *Nature* **395**, 777–780 (1998).
- McKinnon, W. B. Mystery of Callisto: is it undifferentiated? *Icarus* **130**, 540–543 (1997).
- Qi, C., Stern, L. A., Pathare, A., Durham, W. B. & Goldsby, D. L. Inhibition of grain boundary sliding in fine-grained ice by intergranular particles: implications for planetary ice masses. *Geophys. Res. Lett.* **45**, 12757–12765 (2018).
- Stoll, N., Eichler, J., Hörhold, M., Shigeyama, W. & Weikusat, I. A review of the microstructural location of impurities in polar ice and their impacts on deformation. *Front. Earth Sci.* **8**, 615613 (2021).
- Sori, M. M. et al. The vanishing cryovolcanoes of Ceres. *Geophys. Res. Lett.* **44**, 1243–1250 (2017).
- Park, R. S. et al. Evidence of non-uniform crust of Ceres from Dawn's high-resolution gravity data. *Nat. Astron.* **4**, 748–755 (2020).
- Anderson, A. M. & Worster, M. G. Freezing colloidal suspensions: periodic ice lenses and compaction. *J. Fluid Mech.* **758**, 786–808 (2014).
- Rempel, A. W. Formation of ice lenses and frost heave. *J. Geophys. Res. Earth Surf.* **112**, F02S21 (2007).
- Santibáñez, P. A. et al. Differential incorporation of bacteria, organic matter, and inorganic ions into lake ice during ice formation. *J. Geophys. Res. Biogeosci.* **124**, 585–600 (2019).
- Cullen, D. & Baker, I. Observation of impurities in ice. *Microsc. Res. Tech.* **55**, 198–207 (2001).
- Zolotov, M. Y. The composition and structure of Ceres' interior. *Icarus* **335**, 113404 (2020).
- Sori, M. M. et al. Cryovolcanic rates on Ceres revealed by topography. *Nat. Astron.* **2**, 946–950 (2018).
- Bland, M. T. et al. Dome formation on Ceres by solid-state flow analogous to terrestrial salt tectonics. *Nat. Geosci.* **12**, 797–801 (2019).
- Marchi, S. et al. The missing large impact craters on Ceres. *Nat. Commun.* **7**, 12257 (2016).
- Castillo-Rogez, J. C. et al. Ceres: astrobiological target and possible ocean world. *Astrobiology* **20**, 269–291 (2020).
- Castillo-Rogez, J. et al. Science drivers for the future exploration of Ceres: from solar system evolution to ocean world science. *Planet. Sci. J.* **3**, 64 (2022).
- Castillo-Rogez, J. et al. Concepts for the future exploration of dwarf planet Ceres' habitability. *Planet. Sci. J.* **3**, 41 (2022).
- Melosh, H. J. *Impact Cratering: A Geologic Process* (Oxford Univ. Press, 1989).
- Petrenko, V. F. & Whitworth, R. W. *Physics of Ice* (Oxford Univ. Press, 1999).
- Turcotte, D. L. & Schubert, G. *Geodynamics* (Cambridge Univ. Press, 2002).
- Durham, W. B., Kirby, S. H. & Stern, L. A. Creep of water ices at planetary conditions: a compilation. *J. Geophys. Res. Planets* **102**, 16293–16302 (1997).
- Goldsby, D. L. & Kohlstedt, D. L. Superplastic deformation of ice: experimental observations. *J. Geophys. Res. Solid Earth* **106**, 11017–11030 (2001).

## Acknowledgements

This work was funded by NASA Discovery Data Analysis Program (DDAP) grant 80NSSC22K1062, which was received by all authors.

## Author contributions

I.F.P. created and ran the finite element method simulations and led the writing of the manuscript. All authors conceptualized the study and edited the manuscript.

## Competing interests

The authors declare no competing interests.

## Additional information

**Supplementary information** The online version contains supplementary material available at <https://doi.org/10.1038/s41550-024-02350-4>.

**Correspondence and requests for materials** should be addressed to I. F. Pamerleau.

**Peer review information** *Nature Astronomy* thanks Lauren Schurmeier and the other, anonymous, reviewer(s) for their contribution to the peer review of this work.

**Reprints and permissions information** is available at [www.nature.com/reprints](http://www.nature.com/reprints).

**Publisher's note** Springer Nature remains neutral with regard to jurisdictional claims in published maps and institutional affiliations.

**Open Access** This article is licensed under a Creative Commons Attribution-NonCommercial-NoDerivatives 4.0 International License, which permits any non-commercial use, sharing, distribution and reproduction in any medium or format, as long as you give appropriate credit to the original author(s) and the source, provide a link to the Creative Commons licence, and indicate if you modified the licensed material. You do not have permission under this licence to share adapted material derived from this article or parts of it. The images or other third party material in this article are included in the article's Creative Commons licence, unless indicated otherwise in a credit line to the material. If material is not included in the article's Creative Commons licence and your intended use is not permitted by statutory regulation or exceeds the permitted use, you will need to obtain permission directly from the copyright holder. To view a copy of this licence, visit <http://creativecommons.org/licenses/by-nc-nd/4.0/>.

© The Author(s) 2024